

MODIFICATIONS OF THE FUEL ROD ANALYSIS PROGRAM FRAP-S3 TO ACCOUNT FOR THE EFFECTS OF FUEL INITIAL DENSITY

J. YAUNG and N. GHONIEM
 University of California at Los Angeles
 School of Engineering and Applied Science
 Los Angeles, California 90024

Received July 28, 1980

Accepted for Publication January 19, 1981

The Fuel Rod Analysis Program (FRAP-S3) is a fairly comprehensive computer code that is developed for the analysis of light water reactor fuel elements during steady-state operation. However, the code predicts an increase in the fuel radial temperature distribution with an increase in the fuel density, which is contrary to experiments. A simple modification of the code was used where the thermal conductivity is treated as porosity independent in the inner iteration loops of the program. The resulting temperature profile is corrected for the effects of porosity after it has converged. The modified code shows good agreement with the IFA-11 series of experiments using the Halden Boiling Water Reactor in Sweden.

INTRODUCTION

The Fuel Rod Analysis Program-Steady State, Version 3 (FRAP-S3) (Ref. 1) is a FORTRAN IV computer code developed to describe the steady-state and long-term burnup response of oxide fuel rods in light water reactors. In addition, the code is designed to generate parametric data required as initial conditions for transient accident analysis using versions of the transient analysis code FRAP-T (Ref. 2).

Recently, Kerrigan and Coleman³ studied the FRAP-S3 burnup-dependent distributions of fuel stored energy using uncertainty analysis. When utilizing statistical methods for input-output studies, it is important to verify the trends in the code predictions as compared to experimental data. An investigation of the effects of changes in the initial fuel density on the fuel element thermal behavior is an

important part of the assessment of any fuel element modeling code. In this paper, we describe simple modifications to FRAP-S3 that result in better correlations with experimental data. The effects of the fuel initial density on its radial temperature distribution are evaluated.

EXPERIMENT DESCRIPTION

The IFA-11 series of experiments was conducted using the Halden Boiling Water Reactor in Sweden. Five fuel pin centerline temperatures were measured under the same system conditions (inlet temperature, system pressure, etc.). Three of the fuel pins (HBA, HBB, HBC) were particularly interesting to evaluate because of differences in their gap size, density, and burnup. While the important specifications of the three fuel pins are listed below, a full account of the IFA-11 experiment is given in Ref. 4. A summary of the results relevant to our work is given in Fig. 1 and Table I.

Figure 1 shows the centerline temperatures plotted as functions of the peak linear power for HBA, HBB, and HBC. From the figure, two observations can be noticed. The first is the effect of the fuel initial density, where the results indicate that the higher initial density fuel pin (HBA) shows a lower centerline temperature at the same heat load. The second is related to the initial fuel cladding gap size. It is clearly shown that a larger gap size (HBC) has the effect of increasing the centerline temperature, even though the initial fuel density remains the same between HBB and HBC.

FRAP-S3 PREDICTIONS

The FRAP-S3 contains two different gap conductance models. The first is based on a cracked pellet

TABLE I
 Summary of Relevant Results

Fuel Data	HBA	HBB	HBC
Fuel form	5% enriched sintered UO ₂ pellets		
Cladding material	Zircaloy-2		
Density (g/cm ³)	10.70 (97.54% TD ^a)	10.45 (95.26% TD)	10.47 (95.4% TD)
Pellet diameter (mm)	12.54	12.54	12.43
Diameter clearance (mm)	0.05 ± 0.01	0.06 ± 0.01	0.17 ± 0.01

^aTD = theoretical density.

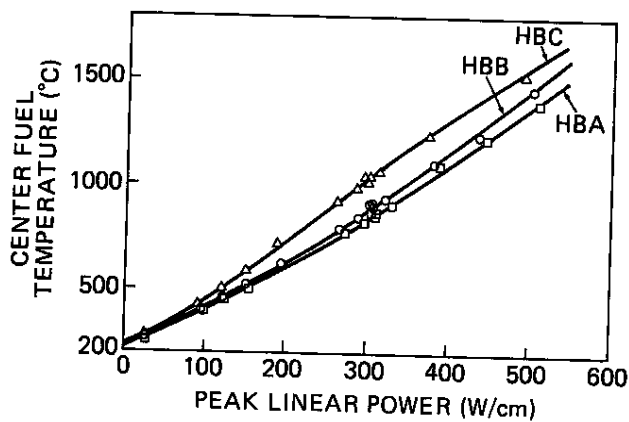


Fig. 1. Centerline temperature in IFA-11 HBA: gap = 0.05 mm, $\rho = 97.5\%$ TD; HBB: gap = 0.05 mm, $\rho = 95.4\%$ TD; HBC: gap = 0.17 mm, $\rho = 95.4\%$ TD. 100% TD = 10.97 g/cm³.

model¹ and the second, which is the annular gap model, is a modification of the Ross and Stoute⁵ formulation.

The models have been compared with experimental data to determine the correct values of the various constants.

To study the systematic trends in the code predictions, a parametric study of the effects of fuel initial density was performed for the conditions of the HBC fuel pin. The significant parameters of some computer runs for the annular gap model are listed in Table II while the cracked pellet model gave similar trends. Centerline temperature, fuel surface temperature, fuel cladding gap temperature drop, and the gap conductance are shown for 93, 95.4, and 98% TD during the beginning-of-life (BOL) power ramping of the HBC case.

Table II shows two different problems with the code predictions that do not reflect the trends in the experimental measurements. An increase in the fuel density is shown to give rise to an increase in the

fuel centerline temperature. This particular behavior, which is opposite to experimental observations, is shown to hold for the two investigated gap conductance models. The second discrepancy is observed when comparing the fuel surface temperatures of the three chosen densities. Since the coolant flow conditions are assumed to be held the same for the three cases, and the gap conductance is about constant in the power range of 8.77 to 15.36 kW/ft, it is surprising to notice an increase in the fuel surface temperature with higher fuel density. Note that the three different sets of calculated results in Table II for the same peak linear power (15.36 kW/ft) show the effect of fuel burnup at a constant power level.

The fuel density changes are accounted for in FRAP-S3 by using a porosity factor to correct for deviations from a standard density of 95% TD. In the program, the conductivity integral contains the porosity factor inside temperature and mechanical convergence iteration loops. Analysis of FRAP-S3 temperature predictions indicated that the relocation model does not properly account for porosity effects resulting in erroneous surface temperatures. The errors propagate through conductivity integrals⁶ from one power level to the next and accumulate giving rise to a higher centerline temperature for a higher fuel initial density.

MODIFICATIONS OF THE FRAP-S3 COMPUTER CODE

The data base for the fuel element thermal performance in FRAP-S3 is chosen for a fuel density of 95% TD, and therefore the results are expected to be more realistic for densities that are close to 95% TD. This has been shown by the success of the program to simulate the HBB and HBC fuel pin results more closely than the HBA case as is discussed later in detail. We have adopted a rather simple approach, keeping in mind the consistency of the code predictions with experiments as the objective.

TABLE II

Annular Gap Model Thermal Parameters for the HBC Fuel Pin

Time Period (h)	Power (kW/ft)	Center Temperature (°F)			Surface Temperature (°F)			Gap Temperature Drop (°F)			Gap Conductance (Btu/h·ft ² ·°F)		
		Fuel Theoretical Density											
		93%	95.4%	98%	93%	95.4%	98%	93%	95.4%	98%	93%	95.4%	98%
0.1 - 1.25	2.48	768	835	906	514	555	598	17	58	101	1006	1063	1133
1.25- 3.03	6.07	1290	1401	1519	571	609	648	53	90	129	1557	1771	2072
3.03- 4.37	8.77	1703	1835	1971	572	620	672	38	86	138	2643	2671	2692
4.37- 5.34	10.71	1993	2142	2296	594	645	701	49	100	156	2715	2726	2733
5.34- 6.33	12.71	2301	2466	2634	619	673	732	64	118	177	2767	2761	2755
6.33- 7.65	15.36	2690	2880	3089	652	710	774	83	141	204	2812	2798	2784
7.65- 588	15.36	2757	2940	3225	691	751	840	121	181	267	1937	1958	1927
588 -1168	15.36	2975	3099	3300	739	800	879	169	230	309	1614	1654	1647

As a first step, the porosity factor, f_p , was removed from the conductivity expressions. The fuel conductivity expressions of MATPRO-9 are given as⁷

$$k = \frac{[1 - \beta(1 - D)]}{[1 - \beta(1 - 0.95)]} \left[\frac{k_1}{k_2 + T} + k_3 \exp(k_4 T) \right] \quad (0^\circ\text{C} < T \leq 1650^\circ\text{C}) \quad (1)$$

and

$$k = \frac{[1 - \beta(1 - D)]}{[1 - \beta(1 - 0.95)]} [k_5 + k_3 \exp(k_4 T)] \quad (1650^\circ\text{C} \leq T \leq 2840^\circ\text{C}) \quad (2)$$

where

$k_1, k_2, k_3, k_4,$ and $k_5 = \text{constants}$

$$\beta = 2.58 - 0.58 \times 10^{-3} T \quad (3)$$

$D = \text{fractional theoretical density.}$

In the present approach to the problem, the temperature distribution across the fuel element was assumed to take the general form

$$T_R(r) - T_s = \frac{\phi(r)}{k_R [T_R(r)]} \quad (4)$$

where $\phi(r)$ is an unspecified function of the radial position (r) and k_R is a temperature-dependent reference conductivity. In the special case of a temperature-independent conductivity, the function $\phi(r)$ takes the form

$$\phi(r) = \frac{HR^2}{4} \left(1 - \frac{r^2}{R^2} \right) \quad (5)$$

where R is the fuel rod inner radius, and H is the volumetric heat generation rate.

Now assume that $T_R(r)$ is the reference temperature distribution calculated for k_R at $D = 0.95$. If one is interested in evaluating the temperature distribution, $T(r)$, at any other conductivity $k = f_p k_R$, Eq. (4) is again assumed to hold. Therefore, the new temperature distribution is given by

$$T(r) - T_s = \frac{\phi(r)}{f_p k_R [T(r)]} \quad (6)$$

where f_p is a porosity factor that is given by

$$f_p = \frac{[1 - \beta(1 - D)]}{[1 - \beta(1 - 0.95)]} \quad (7)$$

Dividing Eq. (6) by Eq. (4), we obtain an approximate value of the temperature distribution evaluated at any density, from that computed at 95% TD:

$$T(r) = T_s + \frac{1}{f_p} [T_R(r) - T_s] \quad (8)$$

Equation (8) is then used as a simple basis for modifying the FRAP-S3 computer code. The new version is denoted by FRAP-S3-UCLA. The calculations were first performed for the reference case at $D = 0.9$ and $f_p = 1$, inside the convergence loops, and then Eq. (8) was applied on the resulting temperature distribution.

As a test of the modification and its effects on the correlation with experiments, the IFA-11 series of experiments was simulated with the new version of the code.

CORRELATION WITH EXPERIMENTS

A series of computer runs was performed for the IFA-11 experiments for the fuel pins HBA, HBB, and HBC with the modified FRAP-S3-UCLA. A comparison between the FRAP-S3 version results (S3) and

the present computations (S3-UCLA) is shown in Table III. The HBB and HBC cases showed little change from the FRAP-S3 results, which is to be expected since the density is not very different from the standard of 95% TD. On the contrary, the fuel centerline temperature values of S3-UCLA are shown to be ~10 to 15% lower than those predicted by FRAP-S3 in the HBA case. This is more in line with experimental trends. Note that the centerline temperatures at zero power (3×10^{-5} kW/ft) must be the same as the surface temperatures at thermal equilibrium. The S3-UCLA shows the identical centerline (and surface) temperatures for the same coolant conditions of HBA, HBB, and HBC, while S3 predicts variations in this temperature.

Figure 2 shows the fuel centerline temperature as a function of linear peak power for the HBA case. A

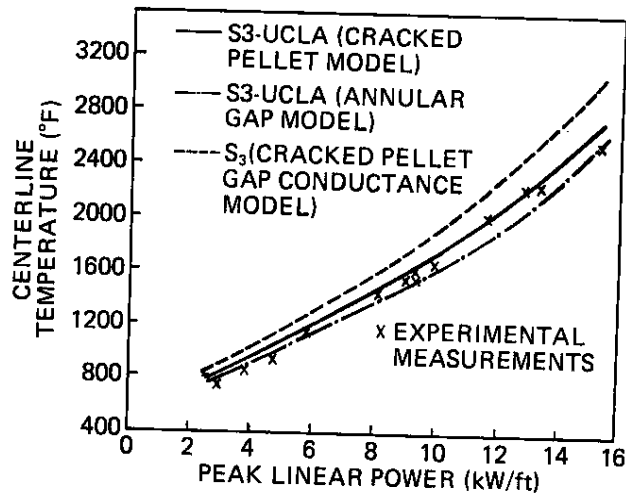


Fig. 2. A comparison of FRAP-S3 results and FRAP-S3-UCLA for the fuel pellet centerline temperature. The comparison is for IFA-11, HBA at BOL.

comparison between the results of FRAP-S3-UCLA is shown along with the measured data points. The new results are shown to be well within the experimental range. The differences between the results of the cracked pellet model and the annular gap model are not as pronounced as in FRAP-S3, as noted in Table III.

Finally, a parametric study of the density effect was conducted by considering two different fuel densities, 93 and 98% TD. This study was performed to investigate the effects of large density variations on the results of the calculations. The input values are those of IFA-11 (HBC) at BOL. Figure 3 indicates that while FRAP-S3 gives a much higher centerline temperature for the 98% TD case compared to 93% TD, the FRAP-S3-UCLA gives exactly the opposite trend. Also, the temperature differences between 93 and 98% TD are shown not to be too drastic. These trends agree qualitatively with experiments.

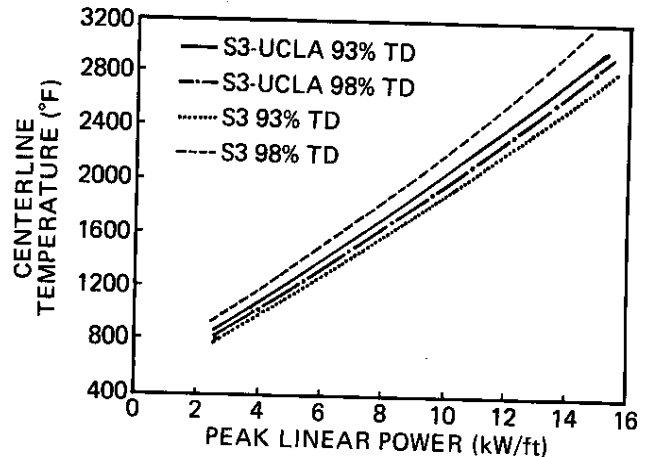


Fig. 3. Effect of fuel density on centerline temperature versus peak linear power for BOL.

TABLE III

A Comparison Between Fuel Centerline Temperatures (°F), Using the FRAP-S3 and the FRAP-S3-UCLA Versions

HBA				HBB				HBC				Linear Power (kW/ft)
Annular		Cracked		Annular		Cracked		Annular		Cracked		
S3-UCLA	S3	S3-UCLA	S3	S3-UCLA	S3	S3-UCLA	S3	S3-UCLA	S3	S3-UCLA	S3	
432	468	432	468	432	435	432	435	432	438	432	438	
729	803	757	833	748	756	774	782	820	835	844	859	2.48
1128	1252	1216	1355	1177	1190	1245	1259	1375	1401	1454	1484	6.07
1435	1614	1531	1698	1503	1520	1609	1619	1802	1835	1920	1952	8.77
1707	1922	1812	2040	1766	1788	1865	1886	2106	2142	2233	2269	10.71
2021	2272	2168	2437	2085	2111	2216	2244	2426	2466	2560	2598	12.71
2490	2788	2710	3031	2560	2591	2759	2792	2837	2880	2972	3018	15.36
2558	2852	2653	2984	2637	2667	2712	2744	2898	2940	2950	2994	15.36
2576	2874	2646	2981	2696	2742	2714	2748	3058	3099	3045	3086	15.36

REFERENCES

1. J. A. DEARIEN et al., "FRAP-S3: A Computer Code for the Steady-State Analysis of Oxide Fuel Rods," TREE-NUREG-1107, U.S. Nuclear Regulatory Commission, EG&G Idaho, Inc. (July 1977).
2. J. A. DEARIEN et al., "FRAP-T4: A Computer Code for the Transient Analysis of Oxide Fuel Rods," CDAP-TR-78-027, U.S. Nuclear Regulatory Commission, EG&G Idaho, Inc. (July 1978).
3. J. D. KERRIGAN and D. K. COLEMAN, "Application of the Response Surface Method of Uncertainty Analysis to Establish Distributions of FRAP-S3 Calculated Stored Energy for PWR-Type Fuels," *Nucl. Eng. Des.*, **54**, 211 (1979).
4. K. D. KNUDSEN and B. M. MAJOR, "A Compilation of Test Fuel Data of the 1964-1966 Test Fuel Program," HPR-81, Halden Boiling Water Reactor Project (Dec. 1967).
5. A. M. ROSS and R. L. STOUTE, "Heat Transfer Coefficient Between C102 and Zircaloy-2," AECL-1552, Atomic Energy of Canada Limited (June 1962).
6. G. BERNA, EG&G Idaho, Inc., Private Communication (1980).
7. P. E. MacDONALD and L. B. THOMPSON, Eds., "MATPRO-VERSION 9, A Handbook of Materials Properties for Use in the Analysis of LWR Fuel Behavior," TREE-NUREG-1005, p. 15, EG&G Idaho, Inc. (1976).